Received: 25 March 2026 | Revised: 14 May 2026 | Accepted: 23 June 2026 | Published online: 20 July 2026

RESEARCH ARTICLE

Journal of Optics and Photonics Research
2026, Vol. 00(00) 1–12
DOI: 10.47852/bonviewJOPR62029761

BON VIEW PUBLISHING

Photo-Stability of Polymethyl Methacrylate Incorporated with Vanillin and Metal Oxide Nanoparticles

Great Iruoghene Edo[1,*], Emad Yousif[1] and Mohammed H. Al-Mashhadani[1]

[1] *Department of Chemistry, Al-Nahrain University, Iraq*

Abstract: The material poly(methyl methacrylate), PMMA, is used for many different purposes, ranging from high-resolution electron beam lithography for microelectronics manufacturing through medical uses such as intraocular lenses and bone cements to the manufacture of automobile taillight covers and as a shatterproof replacement for glass in aquaria, signs, and window coverings. Photostabilization is necessary to protect polymeric materials from photodegradation and photooxidation caused by aging and ultraviolet (UV) radiation. It is imperative, therefore, to modify polymeric compounds for increased resistance against degradation due to extended exposure to UV light. There have been recent advances, which have led to the development of different polymeric materials that can be used as potential photostabilizers. This work focuses on the surface modification of the polymer PMMA through incorporating inorganic metal oxide nanoparticles in the polymer backbone. Upon reacting PMMA with ethylenediamine, an amino group will react with vanillin to produce the respective Schiff's base. Incorporation of nano metal oxides (TiO_2, NiO, and CuO) leads to the formation of inorganic metal oxide nanoparticles into the polymer chains. Films of the treated PMMA were made and subjected to UV irradiation to investigate the effect of the additives on the photostabilization of PMMA. The effects of additives and the type of metal oxide on the photostabilization of PMMA were evaluated by infrared spectroscopy, weight loss, surface morphological investigation, and determination of the rate constant of decomposition. PMMA treated with organic nano metal oxides showed low photodegradation as compared to pure organic-treated PMMA.

Keywords: polymethyl methacrylate, weight loss, ultraviolet irradiation, field emission scanning electron microscopy (FESEM)

1. Introduction

Synthetic polymers have a wide range of applications in contemporary society. For instance, researchers are still interested in organic conducting polymers [1]. Compared to traditional insulating polymeric materials, the polymers have distinct electrical, mechanical, optical, morphological, and crystallinity features, partly because of their extended π-electron conjugation. Additionally, the polymers may be semiconductors with a range of potential applications, including biomedical ones [2]. Moreover, they can be used in the production of dielectric-free substances, solar panels, transducers, rechargeable batteries, super capacitors, and organic light-emitting diodes. The high strength/weight ratio, durability, cost-effectiveness, and ease of processing into films make them ideal for use in various areas. [3]. Due to the increased demand for these items, it is becoming more and more crucial to produce high-performing and environmentally friendly renewable materials [4]. In the instance of polymers, this involves mitigating the detrimental effects of severe weather conditions in order to extend their useful life in outdoor applications [5]. The main causes of the deterioration of polymeric materials are high temperatures, oxygen, high humidity, ultraviolet (UV) radiation, and contaminants [6, 7]. Such exposure results in photooxidation and breakdown of polymer chains by means of scission and cross-linking [8]. The mechanical properties of the polymers become adversely affected, along with surface cracks and discoloration [9]. Improvement in the ability of the polymers to resist photodegradation via additive and surface modification can help prevent such degradation [10]. There are numerous uses for poly(methyl methacrylate) (PMMA) as blends and composites, as well as in pure form [11]. PMMA is widely used in applications such as lenses, dentistry tools, surgery tools, prosthetics, drug delivery devices, and photo-resist materials [12]. The wide usage of PMMA comes as a result of having many desirable qualities, among which are good visibility, low density, high strength and physical properties, cheapness, toughness, and easy manipulation. However, under the presence of oxygen [13], PMMA will decompose and degrade if exposed to extreme temperatures and humidity conditions [14]. PMMA exposed to UV radiation develops holes and cracks, discoloration, and poor durability [15]. Bond cleavage causes the long polymeric chains in PMMA to break down into shorter pieces during the photodegradation process [16]. Chain scission and the generation of free radicals are two aspects of this process's mechanism [17]. The degree of damage to the polymeric materials is associated with the duration of the irradiation time

***Corresponding author:** Great Iruoghene Edo, Department of Chemistry, Al-Nahrain University, Iraq. Email: great.edo@nahrainuniv.edu.iq

[18]. Photodegradation can be effectively decreased by combining polymeric materials with UV inhibitors, including metallic compounds, organics, fibers, and pigments [19]. The level of sunlight stabilization of PMMA is influenced by a number of parameters, such as the size of the materials and the characteristics of the additives [20].

Polymethyl methacrylate (PMMA), often known as acrylic or acrylic glass, is increasingly used in radiation shielding as a lightweight, flexible, and transparent alternative to, or in combination with, traditional shielding materials like glass, concrete, and ceramic. While pure PMMA is not an effective primary gamma shield, it excels at neutron shielding due to its high hydrogen content and can be heavily reinforced with high-atomic-number (high-Z) fillers to create superior shielding [21]. It is possible to create new qualities by blending more than one polymer [22]. For instance, the degree of blending and mixing ability of the component polymers might affect the refractive index as well as other optical characteristics [23]. Properties including mechanical strength, appearance, and transparency can be altered by carefully regulating the concentration and type of blended polymers [24]. The chemistry and degrading characteristics of every kind of molecular species in the mix must be considered. It can be difficult to evaluate how blending affects the base polymer's overall performance; thus, careful structural and optical property evaluation is required [25]. Other techniques, such as surface changes by hydrolysis, aminolysis, and air plasma treatment, have been studied to increase PMMA stability [26]. PMMA can be photostabilized by a number of methods, including chemically modifying the polymeric chains or using additions (such as strongly aromatic metal complexes) [27]. The latter strategy has been shown to be easy to use and successful [28]. In order to increase PMMA's photostability, the current work describes the effective surface modification of PMMA using trisubstituted organotin compounds of a Schiff base with a strongly aromatic moiety [29]. The photostability of plastics has been improved through the application of additives bearing Schiff bases [30]. The process of surface modification on PMMA is a simple, dependable, repeatable, and efficient method for improving PMMA photostability [31]. This paper demonstrates that PMMA can be successfully surface modified with vanillin-metal oxide nanoparticles (NPs) for enhanced photostability.

2. Materials and Methods

2.1. Chemicals

All the chemicals used for analysis were analytical grade. No further purification was done on the chemicals to ensure consistency in purity levels. The chemicals were purchased from Sigma-Aldrich.

2.2. Synthesis of PMMA with ethylenediamine ($H_2N(CH_2)_2NH_2$)

Five grams (5 g) of PMMA were added to 15 mL of a 1:1 (v/v) water/isopropyl alcohol mixture and stirred continuously for 10 min at 25 °C to form a homogeneous solution. The resulting solution was allowed to dry and then submerged in a 15 mL solution of (CH3)2SO (DMSO) and 29.5 g of 1,2-diaminoethane. After refluxing the resulting solution for 1 h while agitating constantly, it was left to air dry for 24 h at 25 °C (Figure 1).

Figure 1
Synthesis of PMMA with ethylenediamine ($H_2N(CH_2)_2NH_2$) and modification of the resulting mixture with vanillin and nanoparticles

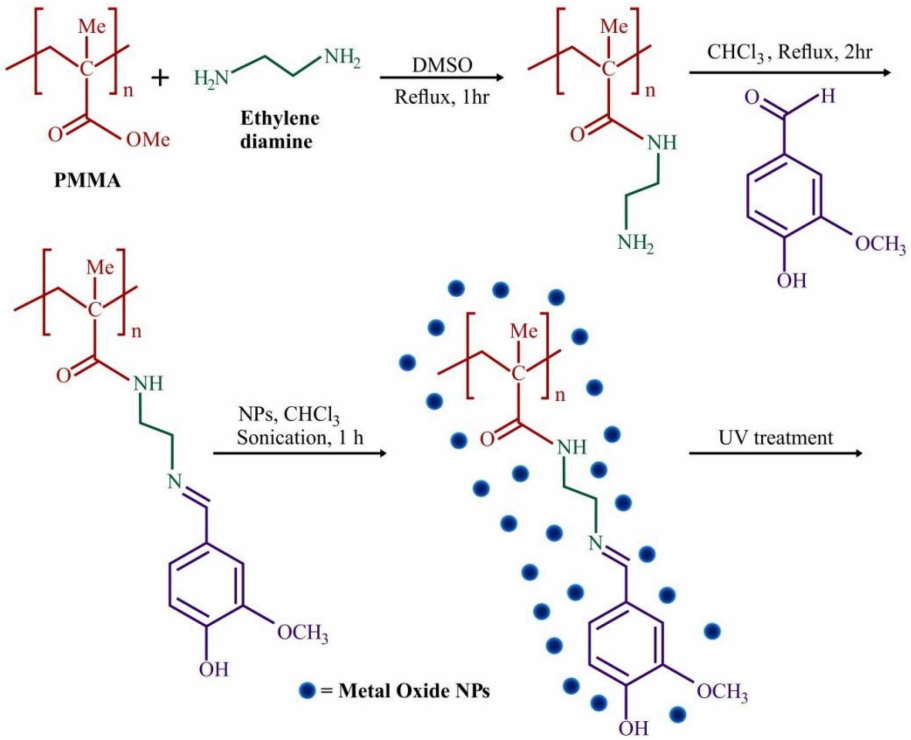

2.3. Modification of PMMA with vanillin (V) and nanoparticles

A small volume of chloroform ($CHCl_3$, 15 mL) was used to dissolve 2.5 g (25 mmol) of PMMA, which was further stirred at 25 °C for 5 min. Vanillin (3.7 g) or 30 mmol of it was then added and stirred again at 55 °C for 2 h. The above process generated PMMA-V after the completion of the evaporation of the solvent for 72 h (Figure 1). Sonication of 5.00 g of PMMA in combination with 0.36 mg of metal oxide NPs (TiO_2, NiO, and CuO) and 100 mL of chloroform for 1 h at room temperature resulted in impregnation of the PMMA-V films with the NPs. Further heating and stirring were performed for 3 h, after which UV analysis was done using the product dissolved into a film with a thickness of approximately 40 μm on a transparent plate (Figure 1). The PMMA is the reference (control) sample. The film described in the text was prepared via drop casting (also referred to as solution or solvent casting). A precise volume of this solution was poured or "cast" directly onto a flat, transparent substrate glass plate. To achieve the specific 40-micrometer thickness, we use a wet film applicator (a Mayer rod) to spread the liquid evenly across the surface. The plate was kept on a level surface to ensure uniformity while the solvent evaporates. This process took place at ambient temperature or in a controlled environment like a hot air oven for 12–24 h to ensure a dry, solid film remains. Once dry, the result is a continuous, transparent film of the specified thickness adhered to the plate, ready for UV–vis spectroscopic analysis. Cross-sectional scanning electron microscope (SEM) imaging was used to directly measure the thickness at the nanometer scale.

2.4. UV-light exposure of modified PMMA (PMMA-V) doped with nanoparticle films

The equipment used was a nickel-plated (MIL-C-23422) plate that had two 40-watt UV fluorescent lamps around its edge. The UV light was applied to the treated films for a maximum of 300 h. The UV irradiation energy at room temperature was 6.2×10^{-9} Einstein·decimeters·mW/area. The horizontal films were placed at a distance of 10 cm from the irradiating sources. The films were exposed to radiation in periods to ensure that radiation reaches all areas equally. After periods of 50 h (which is between 50 h and 300 h), the films were put under analysis. The production and distribution of free radicals, oxygen, and other reacting molecules become easy via the use of exterior defects, ruptures, and cracks, thus affecting the efficiency of the degradation process. As demonstrated in Figure 2, such weaknesses account for the decrease in tensile and load-carrying strength during sample breakage [32].

A qualitative UV Tester (Q-Panel Company, USA) fitted with two 40-watt UVB 365 lamp sources attached to a chrome-plated disc (MIL-C-23422) was used to conduct the UV exposure test. The objectives of the test were to identify the improvement associated with the use of NPs and microparticles and to test the resistance of the films to photodegradation. Particularly, the test was meant to establish the resistance of the films to UV exposure and the improvement brought about by NPs.

2.5. Fourier transform infrared spectroscopy (FTIR) measurement of modified PMMA (PMMA-V) with nanoparticles after exposure to radiation

FTIR spectra were acquired using the Shimadzu FTIR-8300 Spectrophotometer. While irradiating the sample, FTIR spectra

Figure 2
The efficiency of UV-induced polymerization chain disruption

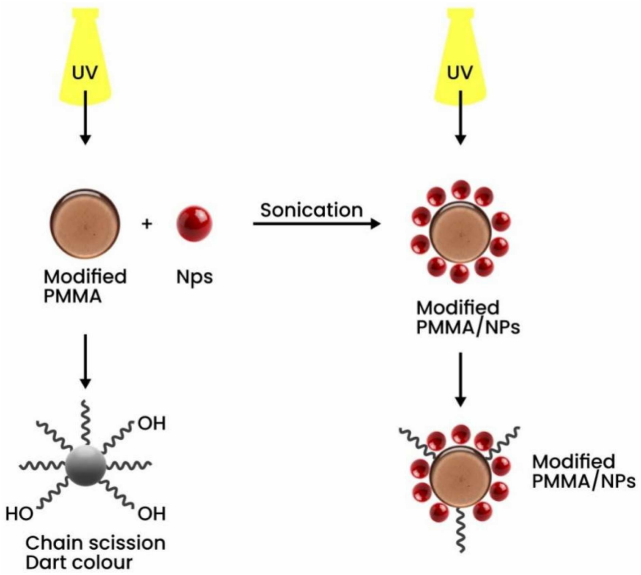

were used to measure the increment of the absorption frequency of bands near the –OH function. Increase in width of the band caused by –OH function (3204 cm^{-1}) was compared with a common band (CH at 1443 cm^{-1}), which is not affected by any irradiation [33]. Index of –OH function (*I*OH) was measured at each irradiation time from the absorbance of –OH and the wavelength of background absorbances (Ar and As). Replicates were done for all measurements, and average results were presented. Index of –OH function (*I*OH) was calculated using Equation (1) from the absorbances of the OH band and reference bands (As and Ar).

$$\mathrm{Is} = \mathrm{As}/\mathrm{Ar} \tag{1}$$

2.6. Weight loss evaluation of modified PMMA (PMMA-V) with nanoparticles after being subjected to UV light

In order to investigate the effect of UV light on the degradation behavior of PMMA-containing materials, sheets of modified PMMA with NPs were measured in terms of weight. The experiment was repeated three times, and the average was taken. Using Equation (2), the ratio of weight loss from PMMA films was calculated by using the initial and final weights.

$$\text{Weight loss (\%)} = \frac{\mathrm{W0} - \mathrm{Wt}}{\mathrm{W0}} \times 100 \tag{2}$$

2.7. Surface morphology characterization by instrumentation analysis: Determination of nanoparticle-doped modified PMMA

Surface morphology studies of the NP-doped modified PMMA material have been done in order to study any irradiation damage by various microscopy instruments. An optical microscope was used to obtain images of the samples of PMMA film [34]. The SEM and atomic force microscopy (AFM) images have been taken by using Veeco (USA) and Carl Zeiss Microscopy's

SIGMA 500 VP, respectively [35]. SEM imaging samples were processed according to the routine procedure [36].

3. Results and Discussion

3.1. Surface modifications of PMMA

When vanillin is converted to vanillin methacrylate and copolymerized with methyl methacrylate, the yield of the insoluble fraction (cross-linked network) is high, often reaching 73–77%. The introduction of metal oxide NPs through *in situ* polymerization techniques combined with cross-linkers like melamine can result in high-yield nanocomposites. While vanillin acts as an additive, it does not significantly alter the primary physical properties, such as flexural strength and modulus, of PMMA. However, the incorporation of NPs generally influences the thermal stability, often leading to a slightly higher melting point or a change in the thermal degradation mechanism. Three sets of aminolysis reactions were conducted to yield amino-functionalized PMMA films. Surface modification of PMMA to obtain an amine-terminated surface using a simple aminolysis method commonly performed to generate amine functionality on the PMMA surface. A polymer was developed in which PMMA was submerged in ethylenediamine solution in dimethyl sulfoxide, where an S_N2 reaction took place and produced an amino-functionalized PMMA surface. The amination of the PMMA surface and the modification of the ester function of PMMA by reaction with vanillin were successfully carried out. The third approach of PMMA surface modification was the reaction of modified PMMA with different nano metal oxides (Figure 1). The physical properties of polymeric materials are presented in Table 1.

3.2. Evaluation of powdered form of PMMA, PMMA modified with vanillin (PMMA + V), using FTIR analysis

The FTIR analysis of the PMMA spectrum showed an entirely novel spectrum at 3280 cm^{-1} (Figure 3). It was determined that the C–N connection was responsible for the emergence of an absorbing band at 1240 cm^{-1}. The C=O (carbonyl-group) and CH=N (imine) in the ester-group caused substantial absorbing peaks to appear in the PMMA at 1730 and 1615 cm^{-1}. The vanillin–N linkages are represented by the freshly formed bands that emerged in the 506–509 cm^{-1} and 442–454 cm^{-1} areas, correspondingly [37] (Figure 3).

The FTIR spectra revealed a broad band with modified PMMA intensities that corresponded to that of the N-H unit located in the ethane-1,2-diamine linkage at 3331–3338 cm^{-1}. Intense and strong bands of absorbance located within the 1731–1733 cm^{-1} area were ascribed to the ester components (carbonyl; C=O group). Around the strong region (1613–1619 cm^{-1}), a strong CH=N interaction was responsible for the significant absorbing spectrum, while within the 1253–1255 cm^{-1} spectrum, the C–N connection was responsible for the band's strength. The C–O stretching resonance of the ester component was observed in the 1205–1208 cm^{-1} area, whereas the C–H stretching vibrating spectrum was observed in the range of 668–988 cm^{-1}.

Table 1
Physical properties of PMMA-based polymers

Polymer	Color	Yield (%)	M.P (°C)
PMMA	White	77	160–162
PMMA/vanillin	Off-white/pale yellow	76	225–227
PMMA/vanillin + TiO_2 NPs	Off-white/yellowish	74	267–269
PMMA/vanillin + NiO NPs	Greenish black	73	285–287
PMMA/vanillin + CuO NPs	Brownish black	75	295–297

Figure 3
FTIR analysis of the powdered form of PMMA, modified with vanillin (PMMA + V)

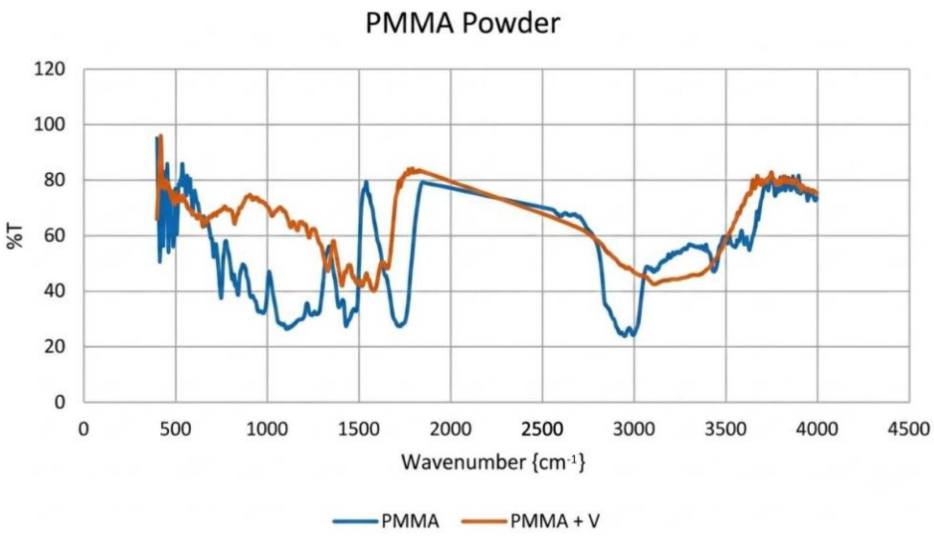

3.3. Evaluation of modified PMMA with vanillin doped with nanoparticles photodegradation using FTIR analysis

PMMA is broken down by photochemistry to produce fragments with particular functional groups, like C=O and –OH units, respectively. By homolytically breaking the C–Me and C–CO_2 Me connections, the reaction produces radicals that are free of charge. An interaction with oxygen that produces peroxy radicals. Hydroperoxides are then created when radicals (peroxyl) that are bonded to the polymer and modified polymer are able to draw radicals (such as hydrogen) from nearby polymerization molecules. When O–OH (such as hydroperoxides) linkages are homolytically broken, alkoxy (which are radicals) are created and attached to the polymerization chain. When radicals (such as hydrogen) are eliminated by the species that are alkoxy radicals, equivalent molecules of alcohol are produced. The O–H group's enhanced absorbing intensity of the band under irradiation was tracked using the FTIR. To be more specific, the O–H absorbance spectrum (at 3206 cm^{-1}) was shown to be stronger when compared to a reference band that is not greatly affected by radiation, like C–H and C–C (at 1445 cm^{-1} and 755 cm^{-1}, respectively). The intensity of the peak differences related to the stretching vibration that occurred in the OH group was noted and contrasted with the standard peak (i.e., C–H). When faced with UV light, the O–H absorbance band's intensity increased, which was an indication of the presence of PMMA degradation by UV.

Figure 4 displays the infrared spectra of the untreated and irradiated (300-h) unmodified PMMA sheets, as well as the irradiated PMMA that includes vanillin (also doped with NPs). The spectrum made it abundantly evident that the O–H absorbance spectrum (at 3206 cm^{-1}) was shown to be stronger when compared to a reference band that is not greatly affected by radiation, like C–H and C–C (at 1445 cm^{-1} and 755 cm^{-1}, respectively).

Figure 4
(a) FTIR analysis of the irradiation of PMMA modified with V and doped with nanoparticles at 0 h and (b) FTIR analysis of the irradiation of PMMA modified with V and doped with nanoparticles at 300 h

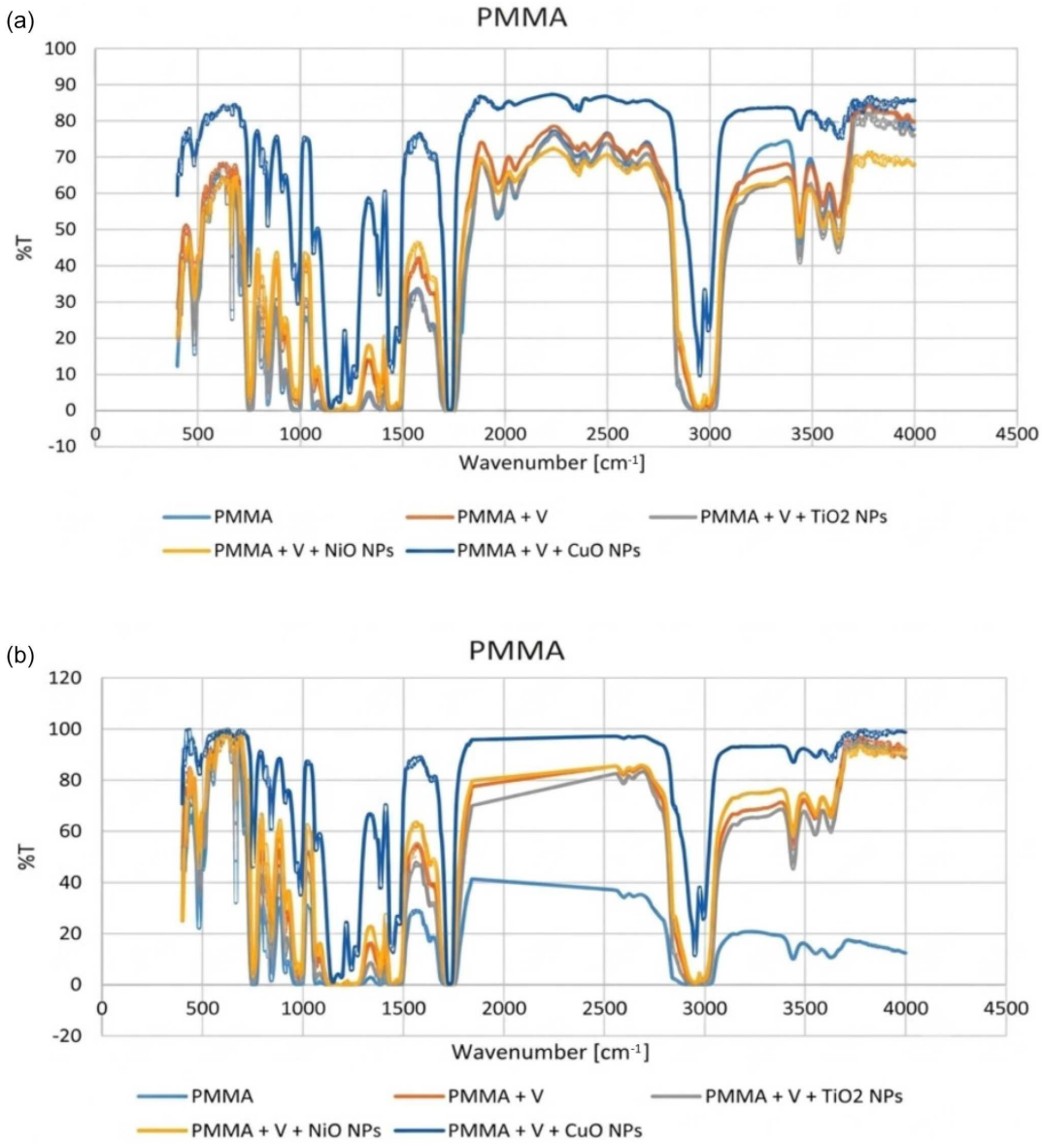

In comparison to the unaltered (pure) film, the intensity of the absorption bands in the PMMA film modified by the vanillin (as well as doped with NPs) was found to be diminished in the specified functional groups. More specifically, it is possible to mention that the film modified by the PMMA, which contained vanillin and was doped with NPs, had less intense absorption bands than the pure one. The effect observed above in the case of PMMA photostabilizers occurs due to the interaction of the ligand with the metal oxide NPs. Owing to the scavenging and basicity of the metal oxide NPs, it is likely for them to operate effectively as PMMA stabilizers. Hardness, electronegativity, and the ratio of charge to the radius are among the factors influencing a tendency of metal to acidification, as it has been shown before [38]. Beyond their basicity, a variety of factors affect metal oxides' NPs ability to operate as PMMA stabilizing agents. Besides the basicity, numerous other variables might affect the ability of metal oxide NPs to act as PMMA stabilizing agents. Such factors as size, thickness, morphology, and chemical composition of NPs might affect the effectiveness of metal oxide NPs as fillers. The ability of metal oxide NPs to modify the PMMA is likely even without their mixing with any compound.

FTIR results indicated significant alterations in the FTIR spectrum as the PMMA sheet was irradiated by the UV light source (λmax = 365 nm). It was evident from the FTIR analysis that new peaks emerged at the 3204 cm^{-1} wavenumber, attributed to the presence of the OH group formed during the process. In the case of the PMMA film presented in Figure 5, the rate of increment in the IOH peak intensity for the aminated PMMA films together with the metal complexes was relatively low.

3.4. Weight loss of irradiated PMMA films

One of the most revealing factors that demonstrates the amount of UV radiation is body weight loss. Figure 6 shows the percentage of weight loss in PMMA films after 300 h of radiation according to Equation (2). Normally, photodegradation caused by sunlight entails weight loss percentage increment. Based on the results obtained, it can be concluded that using the proposed design improves the photostability of PMMA [39]. The reduction in weight rose proportionately to the length of the radiation exposure. The proportion of PMMA films that were left unaltered showed the greatest rise. The polymethyl methacrylate/vanillin initial film excluding NPs had the largest loss of weight percent, while the polymethyl methacrylate/vanillin film containing NPs made from copper oxide had the least percentage of weight loss.

Figure 5
Hydroxyl index (*I*OH) of PMMA films during the irradiation process

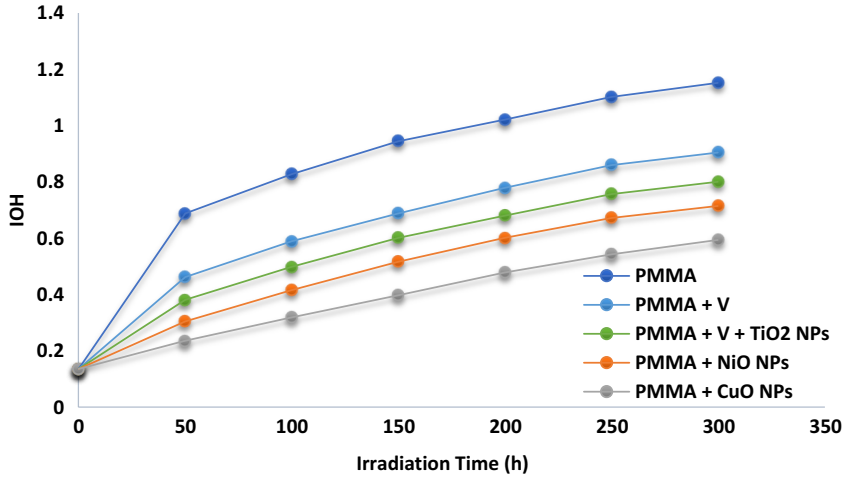

Figure 6
Percentage weight loss of PMMA films during irradiation

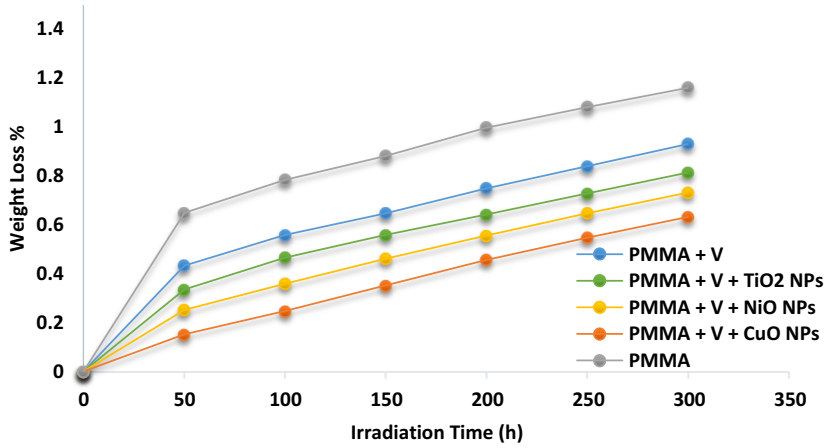

3.5. Evaluation of modified PMMA with vanillin (V) and nanoparticles photodegradation using SEM analysis

The SEM was used to examine the morphology of the PMMA films to produce detailed surface images [40]. Figure 7 shows SEM images of the PMMA films containing vanillin after being subjected to radiation treatment. The figure shows the structure of the radiation-induced PMMA films containing vanillin at 50 and 100 µm resolution. The surfaces of the modified PMMA-vanillin films show better uniformity and improved structure than those of non-modified PMMA films. Figure 8 shows the SEM images of PMMA-V incorporated with TiO_2. The SEM images show an amorphous structure in the PMMA-V-TiO_2 matrix, which is seen at a lower concentration of TiO_2. The foundation of the material composite is its innate disorder. The dispersion of titanium dioxide NPs within the PMMA-V-TiO_2 matrix has been verified by images obtained from SEM. The general amorphous look of the matrix of polymers characterizes the morphology at modest concentration, where the spread tends to appear homogenous. Nevertheless, elevating the titanium dioxide dosage frequently causes the NPs to clump together, which might show up in images from SEM as uneven, fragmented pieces or bunches [41]. Figure 9 shows the SEM images of PMMA-V incorporated with NiO. Sphere-shaped NPs of nickel oxide contained in the uniform PMMA-V matrix of polymers are usually visible in scanning electron microscopic imagery. Usually, the NPs made from nickel oxide show up as separate, frequently spherical or nearly spherical particles. PMMA incorporates the NPs in a continuous, often smooth matrix of polymers. Figure 10 shows the SEM images of PMMA-V incorporated with CuO. Throughout the PMMA-V matrix, these NPs of CuO were visible as separate particles that are inorganic. The PMMA-V matrix contained the CuO NPs in an equal distribution. For constant material qualities, this is frequently the intended result.

Furthermore, the addition of metal oxide NPs (which could seem as pores) to the altered PMMA films gives the surface new morphological features. These results imply that the PMMA structure on its surface was changed by the incorporation of metal oxide NPs, resulting in a discernible morphology of the surface, which could be seen by an SEM. The metal oxide NPs clearly stuck to the surface based on the SEM imaging. Nevertheless, we had been unable to discern a discernible difference between the outermost surfaces, possibly due to PMMA's unique surface characteristics [42]. Since PMMA has an excessively porous structure, it actually has a large area on its surface. The texture of the surface not only shows the existence of NPs but

Figure 7
FESEM image for PMMA + V at 50 and 100 µm

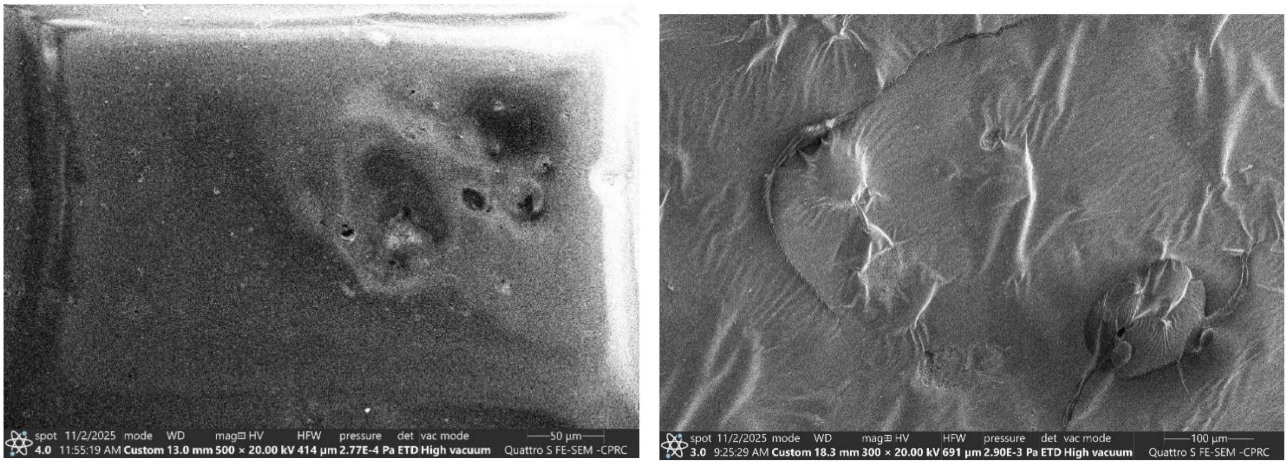

Figure 8
FESEM image for PMMA + V + TiO_2 NPs at 50 and 100 µm

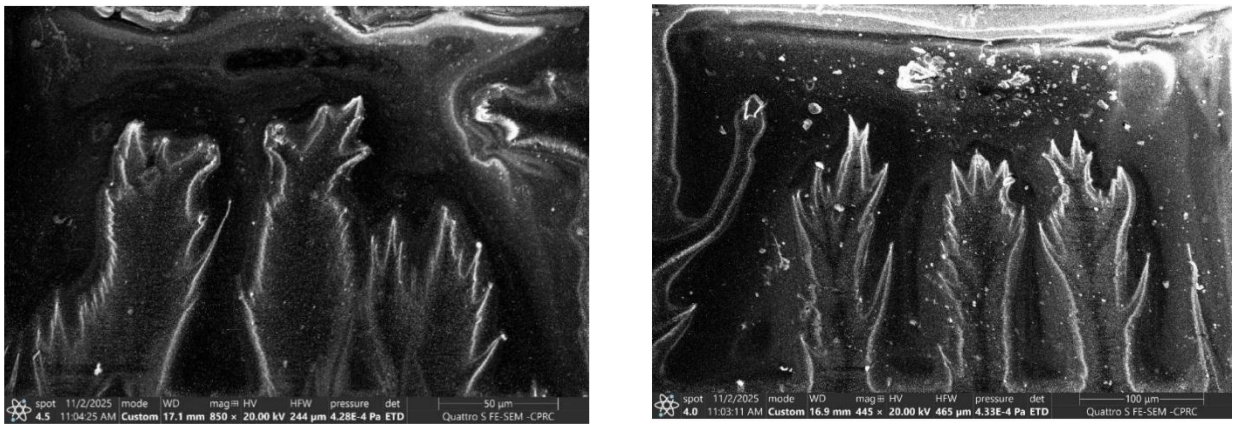

Figure 9
FESEM image for PMMA + V + NiO NPs at 50 and 100 µm

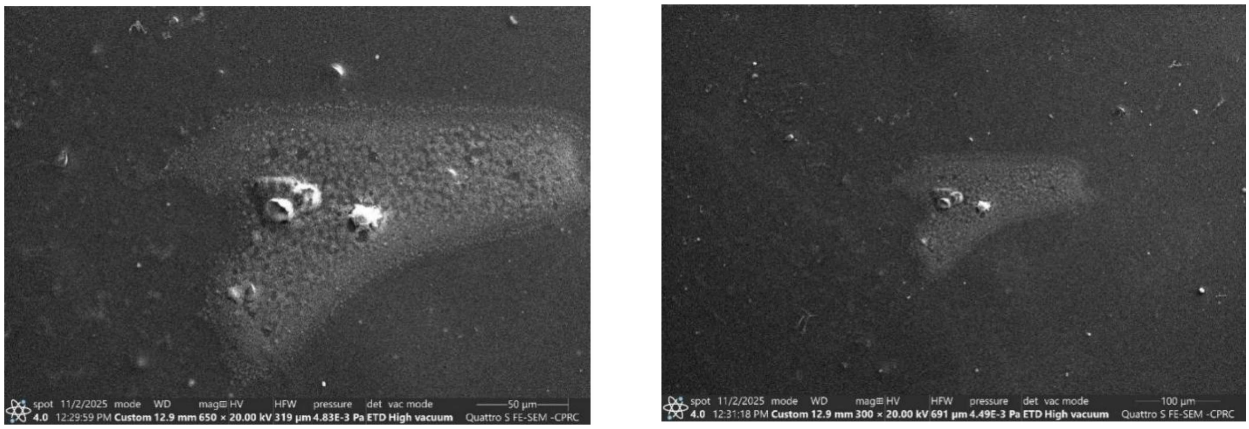

Figure 10
FESEM image for PMMA + V + CuO NPs at 50 and 100 µm

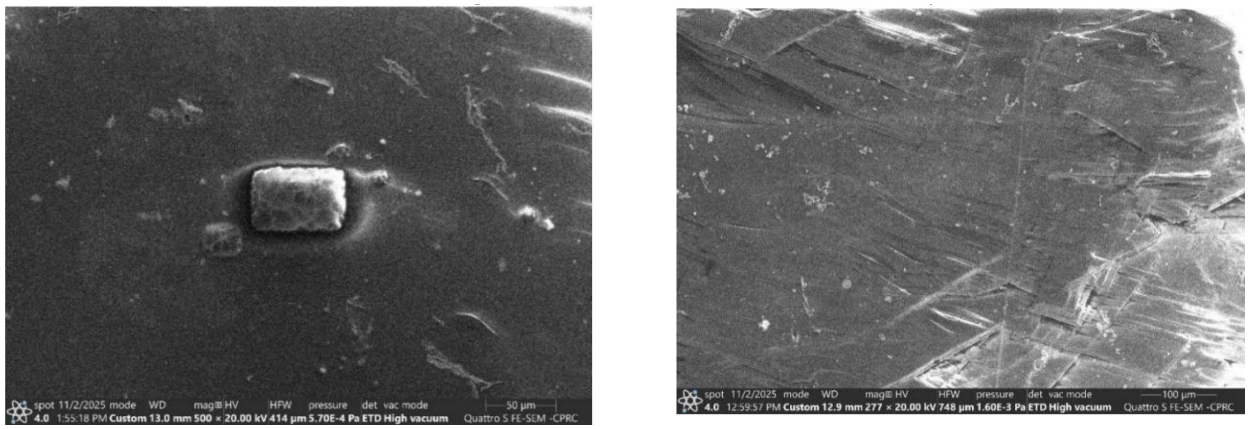

also the outermost irregularity that is probably comparable with respect to the metal oxide NP sizes. This implies the dimensional deterioration brought on by UV radiation at the PMMA material's surface was much lessened when metal oxide NPs were present. In order to study damage caused by radiation, particle aggregation, and particle-size variation using SEM, the following methods were used. Generally speaking, the degradation process leads to weight loss and aggregation as a result of the lack of compatibility of polymers with certain compounds, causing the formation of voids. It can therefore be noted that the process of forming voids can be significantly decreased if pigments are added to polymers and if photodegradation is prevented.

3.6. Evaluation of modified PMMA with vanillin doped with nanoparticles photodegradation using AFM analysis

A complete vacuum is not necessary for AFM, which provides two- and three-dimensional images of the surface structure of the investigated material. This method is simple to use and versatile in its application [43]. Figure 9 shows the two- and three-dimensional AFM images of PMMA incorporated with vanillin under irradiation (300 h). The two- and three-dimensional AFM images given in Figures 11–14 show the effect of irradiation of the PMMA film. From the two- and three-dimensional AFM images of the surface of PMMA films having vanillin and doped with nano metal oxides after irradiation, one can observe that there is a very smooth surface with a minimum roughness factor. On the other hand, the surface was found to be rough for PMMA/Schiff base films. It can be presumed that bond cleavage causes the rough surface of the PMMA film having vanillin and nano metal oxides after irradiation [44]. From Table 2, it can be seen that the roughness factor (Rq; nm) value is maximum for the blank PMMA (285.1 nm) and minimum for the vanillin and CuO NP films (45.5 nm). Figure 12 shows the AFM images of PMMA-V incorporated with TiO_2 NPs. The PMMA-V polymer is filled with titanium dioxide NPs. A uniform surface with tiny, uniformly spaced features is the outcome of a good dispersion, which is frequently made possible by vanillin's involvement [45]. Agglomerations, or massive clumps of TiO_2, are indicated by limited dispersal. In contrast to pure PMMA, which has no additives, the addition of vanillin and titanium dioxide alters the texture. The impact is dependent on concentration. Figure 13 shows the AFM images of PMMA-V incorporated with NiO NPs. During the film-making process, vanillin functions as a porous substance or pore-building component, which results in the creation of tiny or nano-scale spaces or a structure resembling a sponge, altering the whole texture of the exterior. NiO NPs are scattered throughout the matrix of PMMA-V polymer. Vanillin's polar structures may increase stability, which could result in an increasingly uniform AFM image by distributing smaller nickel oxide structures more uniformly. Figure 14 shows the AFM images of PMMA-V

Figure 11
AFM images of irradiated PMMA + V film

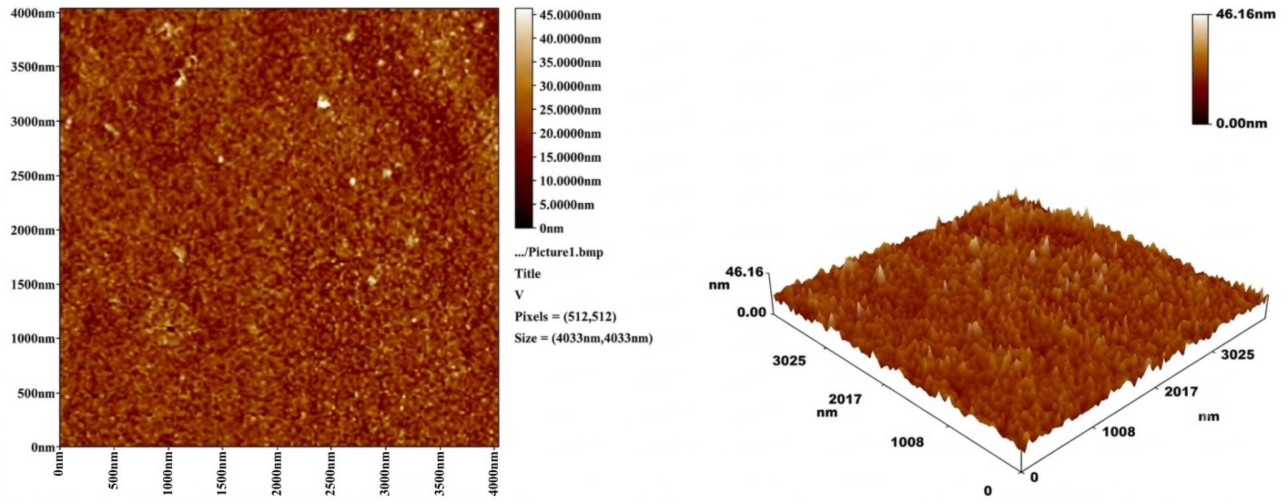

Figure 12
AFM images of irradiated PMMA + V + TiO_2 NPs film

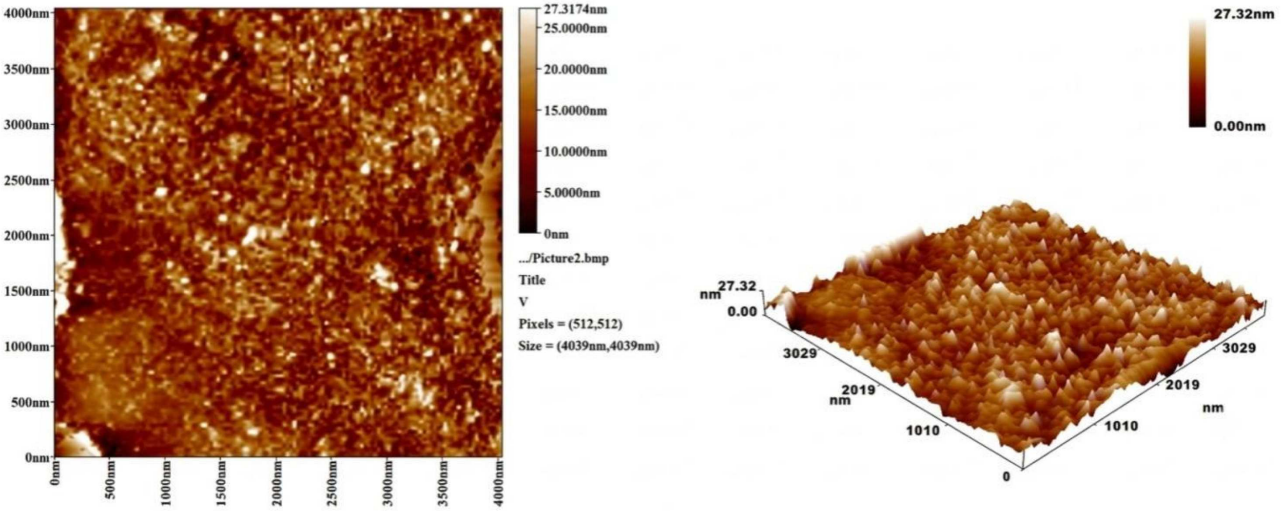

Figure 13
AFM images of irradiated PMMA + V + NiO NPs film

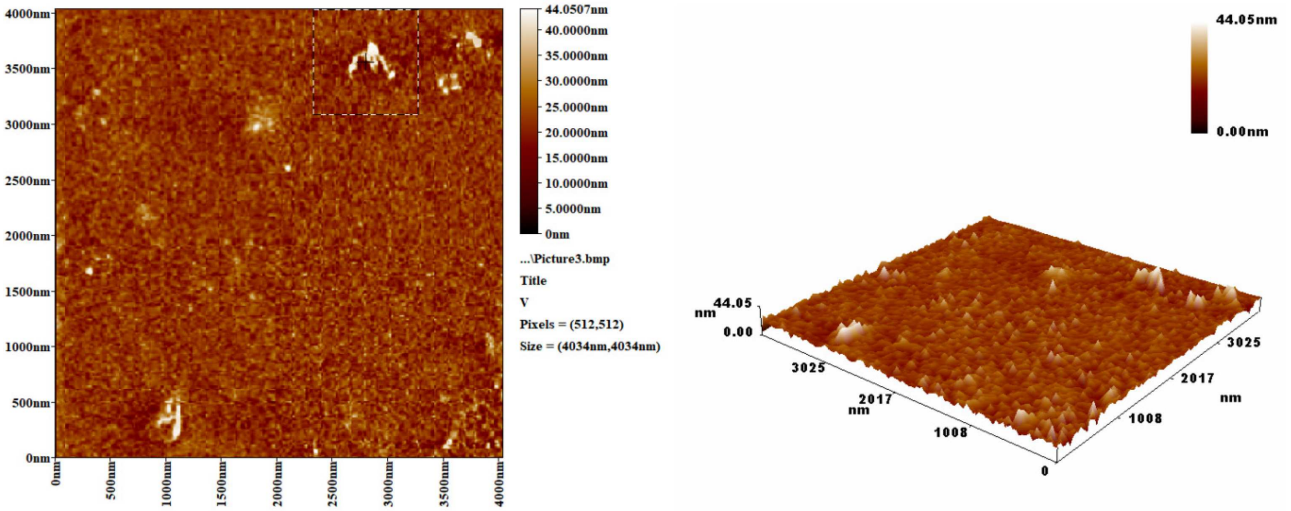

Figure 14
AFM images of irradiated PMMA + V + CuO NPs film

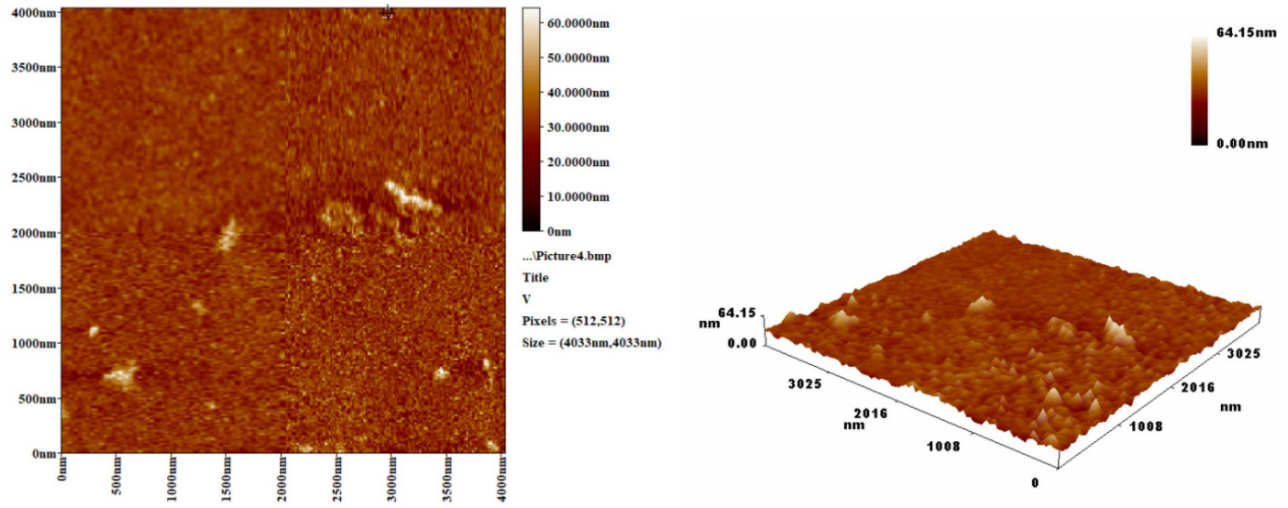

Table 2
Roughness factor (Rq; nm) of PMMA films subjected to radiation exposure (300 h)

Film	Rq (nm)
PMMA	285.1
PMMA + V	126.4
PMMA + V + TiO_2 NPs	88.1
PMMA + V + NiO NPs	51.7
PMMA + V + CuO NPs	45.5

incorporated with CuO NPs. The total roughness on the surface of the film is increased by the incorporation of NPs made from which produce distinctive characteristics that manifest as elevated dots or aggregates. Significant, noticeable "bubbles" or bunches in the AFM photos are indicative of poor copper oxide NPs dispersal and accumulation, which may have a detrimental effect on the tensile and visual characteristics of the nanocomposite. In the darker, thinner, and finer PMMA-v-CuO matrix of polymers, the copper oxide NPs—which are usually round, depending on the synthesis process—show up as elevated characteristics or prominent spots.

4. Conclusion

The surface modification of PMMA was successful, in which inorganic metal oxide NPs have been incorporated. The modified polymeric materials were capable of reducing the harmful effects of UV irradiation. PMMA containing vanillin doped with copper oxide NPs showed the most stabilization effect against photodegradation. The most destructive changes in PMMA have been seen when vanillin was incorporated within the polymeric chains without any metals. The efficiency of metal oxides' stabilizing effect for PMMA is decreasing in the following order: copper oxide, nickel oxide, and titanium oxide NPs. It should be highlighted that the surface modification of PMMA led to an essential decrease in photolysis reaction rate. This modification made it possible for PMMA to lessen the damaging effects of UV radiation with an emission wavelength of 365 nm for as many as 300 h. When compared to the unmodified films, the ability to absorb light of the polymer was significantly improved in the modified films. Interface disintegration was negligible in PMMA-based samples containing vanillin and NPs made from copper oxide.

Ethical Statement

This study does not contain any studies with human or animal subjects performed by any of the authors.

Conflicts of Interest

The authors declare that they have no conflicts of interest to this work.

Data Availability Statement

Data sharing is not applicable to this article as no new data were created or analyzed in this study.

Author Contribution Statement

Great Iruoghene Edo: Conceptualization, Methodology, Software, Validation, Formal analysis, Investigation, Resources, Data curation, Writing – original draft, Writing – review & editing, Visualization, Project administration. **Emad Yousif:** Conceptualization, Methodology, Software, Validation, Resources, Data curation, Writing – review & editing, Visualization, Supervision, Project administration. **Mohammed H. Al-Mashhadani:** Resources, Data curation, Writing – review & editing, Visualization, Supervision, Project administration.

References

[1] Dimassi, S. N., Hahladakis, J. N., Yahia, M. N. D., Ahmad, M. I., Sayadi, S., & Al-Ghouti, M. A. (2022). Degradation-fragmentation of marine plastic waste and their environmental implications: A critical review. *Arabian Journal of Chemistry*, *15*(11), 104262. https://doi.org/10.1016/j.arabjc.2022.104262

[2] Hasan, M. B., Parvez, M. M., Abir, A. Y., & Ahmad, M. F. (2025). A review on conducting organic polymers: Concepts, applications, and potential environmental benefits. *Heliyon*, *11*(3), e42375. https://doi.org/10.1016/j.heliyon.2025.e42375

[3] Karpiński, R., Przekora, A., & Szabelski, J. (2026). PMMA-based composite bone cements with zirconium oxide fillers of different granulations: Structural optimization and biofunctional potential. *Frontiers in Bioengineering and Biotechnology*, *14*, 1796706. https://doi.org/10.3389/fbioe.2026.1796706

[4] Megahed, O. N., Abdelhamid, M. I., Elwassefy, N. A., Youssef, A. M., El-Damarawi, G., & Bakr, N. A. (2026). Fabrication and characterization of poly methyl methacrylate (PMMA) matrix modified with strontium nanorods. *Scientific Reports*, *16*(1), 9342. https://doi.org/10.1038/s41598-026-39521-4

[5] Maraveas, C., Kyrtopoulos, I. V., Arvanitis, K. G., & Bartzanas, T. (2024). The aging of polymers under electromagnetic radiation. *Polymers*, *16*(5), 689. https://doi.org/10.3390/polym16050689

[6] Beena Unni, A., & Muringayil Joseph, T. (2024). Enhancing polymer sustainability: Eco-conscious strategies. *Polymers*, *16*(13), 1769. https://doi.org/10.3390/polym16131769

[7] Laxmayyaguddi, Y., Chapi, S., & Nandihalli, N. (2025). Electron beam irradiation's effect on polyaniline/$LiClO_4$/CuO nanocomposite: A study of dielectric, conductivity and electrochemical properties. *Applied Sciences*, *15*(7), 4001. https://doi.org/10.3390/app15074001

[8] Edah, G. O., Atiba, J. O., & Fayomi, O. S. I. (2025). Advancements in fibre-reinforced polymers: Properties, applications (A mini review). *Next Materials*, *8*, 100743. https://doi.org/10.1016/j.nxmate.2025.100743

[9] Przesławski, G., Szcześniak, K., Gajewski, P., & Marcinkowska, A. (2022). Influence of initiator concentration on the polymerization course of methacrylate bone cement. *Polymers*, *14*(22), 5005. https://doi.org/10.3390/polym14225005

[10] Ballard, N., Veloso, A., & Asua, J. M. (2018). Mid-chain radical migration in the radical polymerization of n-butyl acrylate. *Polymers*, *10*(7), 765. https://doi.org/10.3390/polym10070765

[11] Abu Hassan Shaari, H., Ramli, M. M., Mohtar, M. N., Abdul Rahman, N., & Ahmad, A. (2021). Synthesis and conductivity studies of poly(methyl methacrylate) (PMMA) by co-polymerization and blending with polyaniline (PANi). *Polymers*, *13*(12), 1939. https://doi.org/10.3390/polym13121939

[12] Yang, S., Karve, V. V., Justin, A., Kochetygov, I., Espín, J., Asgari, M., . . . , & Queen, W. L. (2021). Enhancing MOF performance through the introduction of polymer guests. *Coordination Chemistry Reviews*, *427*, 213525. https://doi.org/10.1016/j.ccr.2020.213525

[13] Ivanova, S., Tomova, Z., Vlahova, A., Stoeva, I. L., Vasileva, E., Uzunova, Y., . . . , & Chonin, A. (2026). Contemporary use of polymers in dentistry: A narrative review. *Polymers*, *18*(1), 138. https://doi.org/10.3390/polym18010138

[14] Andrady, A. L., Heikkilä, A. M., Pandey, K. K., Bruckman, L. S., White, C. C., Zhu, M., & Zhu, L. (2023). Effects of UV radiation on natural and synthetic materials. *Photochemical & Photobiological Sciences*, *22*(5), 1177–1202. https://doi.org/10.1007/s43630-023-00377-6

[15] Ci, S., Wang, B., Di, C., Wang, M., Zhu, B., & Qiao, K. (2025). Effect of ultraviolet aging on properties of epoxy resin and its pultruded fiber-reinforced composite. *Polymers*, *17*(3), 294. https://doi.org/10.3390/polym17030294

[16] Simič, R., Mandal, J., Zhang, K., & Spencer, N. D. (2021). Oxygen inhibition of free-radical polymerization is the dominant mechanism behind the "mold effect" on hydrogels. *Soft Matter*, *17*(26), 6394–6403. https://doi.org/10.1039/D1SM00395J

[17] Robo, M. T., Collias, D., & Zimmerman, P. M. (2022). Interplay between applied force and radical attack in the mechanochemical chain scission of poly(acrylic acid). *The Journal of Physical Chemistry A*, *126*(4), 521–528. https://doi.org/10.1021/acs.jpca.1c08919

[18] Ofoedu, C. E., You, L., Osuji, C. M., Iwouno, J. O., Kabuo, N. O., Ojukwu, M., . . . , & Korzeniowska, M. (2021). Hydrogen peroxide effects on natural-sourced polysaccharides: Free radical formation/production, degradation process, and reaction mechanism—A critical synopsis. *Foods*, *10*(4), 699. https://doi.org/10.3390/foods10040699

[19] Xia, M., Gao, H., Feng, X., & Liu, X. (2026). Photodegradation mechanisms and anti-aging strategies of wood coatings: A comprehensive review. *Polymers*, *18*(9), 1090. https://doi.org/10.3390/polym18091090

[20] von Hertzberg-Boelch, S. P., Luedemann, M., Rudert, M., & Steinert, A. F. (2022). Pmma bone cement: Antibiotic elution and mechanical properties in the context of clinical use. *Biomedicines*, *10*(8), 1830. https://doi.org/10.3390/biomedicines10081830

[21] Echeweozo, E. O., Kırkbınar, M., Alomairy, S., & Al-Buriahi, M. S. (2025). Gamma radiation and charged particle shielding properties of Polymethyl methacrylate- Bi_2O_3 composite for medical shielding applications: Synthesis and simulation study. *Journal of Radiation Research and Applied Sciences*, *18*(1), 101247. https://doi.org/10.1016/j.jrras.2024.101247

[22] Hung, J.-P., Bai, Y.-W., Hung, C.-Q., & Lee, T.-E. (2019). Biomechanical performance of the cemented hip stem with different surface finish. *Applied Sciences*, *9*(19), 4082. https://doi.org/10.3390/app9194082

[23] Yerliyurt, K., Taşdelen, T. B., Eğri, Ö., & Eğri, S. (2023). Flexural properties of heat-polymerized PMMA denture base resins reinforced with fibers with different characteristics. *Polymers*, *15*(15), 3211. https://doi.org/10.3390/polym15153211

[24] Li, X., Li, L., Zheng, Y., Li, Y., Chen, Z., Xiao, J., . . . , & Xiong, Z. (2023). A study of the compressive behavior of recycled rubber concrete reinforced with hybrid fibers. *Materials*, *16*(13), 4731. https://doi.org/10.3390/ma16134731

[25] Kechagias, J. D., Zaoutsos, S. P., Fountas, N. A., & Vaxevanidis, N. M. (2024). Experimental investigation and neural network development for modeling tensile properties of polymethyl methacrylate (PMMA) filament material. *The International Journal of Advanced Manufacturing Technology*, *134*(9-10), 4387–4398. https://doi.org/10.1007/s00170-024-14402-0

[26] Fernández, A., Redondo, A., Martín-de-León, J., & Cantero, D. (2023). PMMA stability under hydrothermal conditions. *The Journal of Supercritical Fluids*, *198*, 105938. https://doi.org/10.1016/j.supflu.2023.105938

[27] Ceylan, G., Emik, S., Yalcinyuva, T., Sunbuloğlu, E., Bozdag, E., & Unalan, F. (2023). The effects of cross-linking agents on the mechanical properties of poly (methyl methacrylate) resin. *Polymers*, *15*(10), 2387. https://doi.org/10.3390/polym15102387

[28] Chen, J., Garcia, E. S., & Zimmerman, S. C. (2020). Intramolecularly cross-linked polymers: From structure to function with applications as artificial antibodies and artificial enzymes. *Accounts of Chemical Research*, *53*(6), 1244–1256. https://doi.org/10.1021/acs.accounts.0c00178

[29] Ahamad Said, M. N., Hasbullah, N. A., Rosdi, M. R. H., Musa, M. S., Rusli, A., Ariffin, A., & Shafiq, M. D. (2022). Polymerization and applications of poly(methyl methacrylate)–graphene oxide nanocomposites: A review. *ACS Omega*, *7*(51), 47490–47503. https://doi.org/10.1021/acsomega.2c04483

[30] Fang, G., Liu, B., Zhang, W., Khan, A., Riahi, Z., Ezati, P., . . . , & Jafari, S. M. (2025). Schiff base crosslinking in biopolymeric food packaging films: Dynamic covalent chemistry for advanced food preservation systems. *Current Research in Food Science*, *11*, 101213. https://doi.org/10.1016/j.crfs.2025.101213

[31] Yuan, M., Huang, D., & Zhao, Y. (2022). Development of synthesis and application of high molecular weight poly(methyl methacrylate). *Polymers*, *14*(13), 2632. https://doi.org/10.3390/polym14132632

[32] Kavda, S., Golfomitsou, S., & Richardson, E. (2023). Effects of selected solvents on PMMA after prolonged exposure: Unilateral NMR and ATR-FTIR investigations. *Heritage Science*, *11*(1), 63. https://doi.org/10.1186/s40494-023-00881-z

[33] Shanti, R., Hadi, A. N., Salim, Y. S., Chee, S. Y., Ramesh, S., & Ramesh, K. (2017). Degradation of ultra-high molecular weight poly(Methyl methacrylate-co-butyl acrylate-co-acrylic acid) under ultra violet irradiation. *RSC Advances*, *7*(1), 112–120. https://doi.org/10.1039/C6RA25313J

[34] Cui, W., Yang, S., Zhang, X., Zhang, Y., Shao, Y., Li, X., . . . , & Jin, Z. (2022). High wear resistance of ultralow-wear polyethylene with different molecular weights under different contact pressure. *Tribology Letters*, *70*(2), 51. https://doi.org/10.1007/s11249-022-01595-2

[35] Nguyen-Tri, P., Ghassemi, P., Carriere, P., Nanda, S., Assadi, A. A., & Nguyen, D. D. (2020). Recent applications of advanced atomic force microscopy in polymer science: A review. *Polymers*, *12*(5), 1142. https://doi.org/10.3390/polym12051142

[36] Minuti, A. E., Labusca, L., Herea, D.-D., Stoian, G., Chiriac, H., & Lupu, N. (2022). A simple protocol for sample preparation for scanning electron microscopic imaging allows quick screening of nanomaterials adhering to cell surface. *International Journal of Molecular Sciences*, *24*(1), 430. https://doi.org/10.3390/ijms24010430

[37] Sánchez-Vergara, M. E., Hamui, L., Gómez, E., Chans, G. M., & Galván-Hidalgo, J. M. (2021). Design of promising heptacoordinated organotin (IV) complexes-PEDOT: PSS-based composite for new-generation optoelectronic devices applications. *Polymers*, *13*(7), 1023. https://doi.org/10.3390/polym13071023

[38] Alhalili, Z. (2023). Metal oxides nanoparticles: General structural description, chemical, physical, and biological synthesis methods, role in pesticides and heavy metal removal through wastewater treatment. *Molecules*, *28*(7), 3086. https://doi.org/10.3390/molecules28073086

[39] Gomaa, F., Moustapha, M. E., & Mohammed, M. I. (2025). Optical tunable, electrical, thermal stable, and photocatalytic properties of PMMA/Fe_2O_3 nanocomposite films. *Journal of Umm Al-Qura University for Applied Sciences*. https://doi.org/10.1007/s43994-025-00250-5 Advanced online publication

[40] Ariaee, S., Jakobsen, B., Norby, P., Smilgies, D.-M., Almdal, K., & Posselt, D. (2023). Thin film and bulk morphology of PI-PS-PMMA miktoarm star terpolymers with both weakly and strongly segregated arm pairs. *Polymer*, *283*, 126202. https://doi.org/10.1016/j.polymer.2023.126202

[41] Altwair, K., Vuksanović, M. M., Mladenović, I. O., & Heinemann, R. J. (2026). Development of PMMA–silica–alumina nanocomposites for enhanced performance. *Polymers and Polymer Composites*, *34*, 1–15. https://doi.org/10.1177/09673911251414228

[42] Kawano, M., Morimitsu, Y., Liu, Y., Miyata, N., Miyazaki, T., Aoki, H., . . . , & Tanaka, K. (2024). In-plane movement of isolated poly(methacrylate) chains on a hydrophilic solid surface. *Macromolecules*, *57*(14), 6625–6633. https://doi.org/10.1021/acs.macromol.4c00724

[43] Yang, C., Dang, C.-Q., Zhu, W.-L., & Ju, B.-F. (2023). High-speed atomic force microscopy in ultra-precision surface machining and measurement: Challenges, solutions and opportunities. *Surface Science and Technology*, *1*(1), 7. https://doi.org/10.1007/s44251-023-00006-5

[44] Songpanit, M., Boonyarattanakalin, K., Limwichean, S., Lertvanithphol, T., Horprathum, M., Pecharapa, W., & Mekprasart, W. (2023). Structural and optical characterizations of polymethyl methacrylate films with the incorporation of ultrafine SiO_2/TiO_2 composites utilized as self-cleaning surfaces. *Polymers*, *15*(15), 3162. https://doi.org/10.3390/polym15153162

[45] Zhu, Z., Yu, Q., Li, H., Han, F., Guo, Q., Sun, H., . . . , & Li, B. (2023). Vanillin-based functionalization strategy to construct multifunctional microspheres for treating inflammation and regenerating intervertebral disc. *Bioactive Materials*, *28*, 167–182. https://doi.org/10.1016/j.bioactmat.2023.05.005

How to Cite: Edo, G. I., Yousif, E., & H. Al-Mashhadani, M. (2026). Photo-Stability of Polymethyl Methacrylate Incorporated with Vanillin and Metal Oxide Nanoparticles. *Journal of Optics and Photonics Research*. https://doi.org/10.47852/bonviewJOPR62029761